STAT3 Regulation of Citrate Synthase Is Essential during the Initiation of Lymphocyte Cell Growth

Sarah MacPherson, Michael Horkoff, Cleo Gravel, Thomas Hoffmann, Johannes Zuber, Julian J. Lum

May 2017

Cell Reports

STAT3 Regulation of Citrate Synthase Is Essential during the Initiation of Lymphocyte Cell Growth

Graphical Abstract

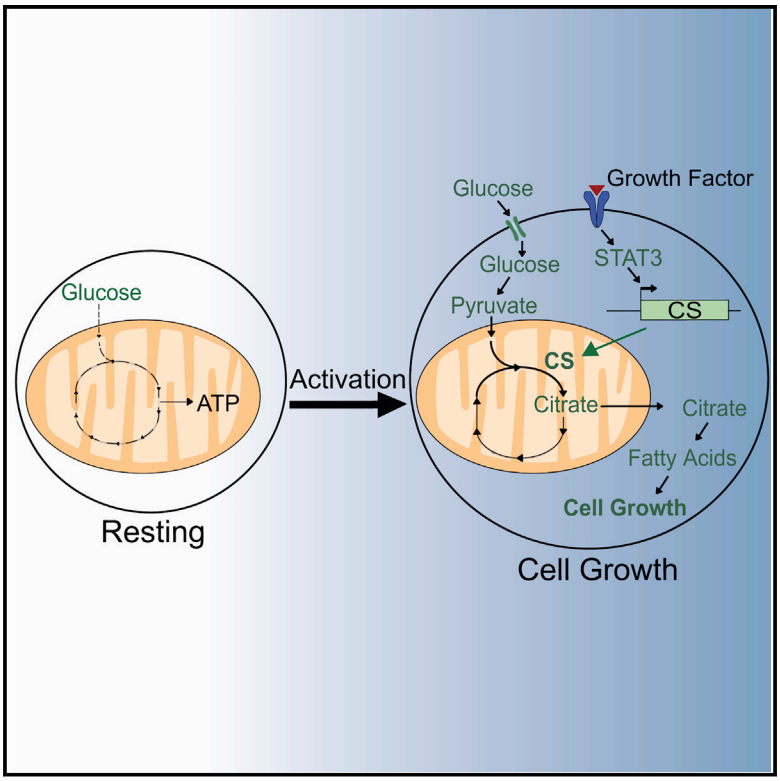

Authors

Sarah MacPherson, Michael Horkoff, Cleo Gravel, Thomas Hoffmann, Johannes Zuber, Julian J. Lum

Correspondence

jjlum@bccancer.bc.ca

In Brief

MacPherson et al. show that STAT3 is required for transcription of citrate synthase during acute stimulation of resting lymphocytes. CS promotes accumulation of intracellular citrate to produce lipids necessary for cell growth. Lymphocytes fail to grow and proliferate without STAT3 or CS following activation, a defect rescued by exogenous citrate.

Highlights

- STAT3 is essential for resting lymphocytes to initiate growth and proliferation
- The metabolic effect of STAT3 is dependent on transcriptional regulation of CS
- Without STAT3, lipid synthesis, growth, and proliferation are blocked
- Growth and proliferation can be rescued by providing exogenous citrate

MacPherson et al., 2017, Cell Reports *19*, 910–918
May 2, 2017
http://dx.doi.org/10.1016/j.celrep.2017.04.012

CellPress

OPEN ACCESS
CellPress

Cell Reports
Report

STAT3 Regulation of Citrate Synthase Is Essential during the Initiation of Lymphocyte Cell Growth

Sarah MacPherson,[1,2] Michael Horkoff,[1,2] Cleo Gravel,[1,2] Thomas Hoffmann,[3] Johannes Zuber,[3] and Julian J. Lum[1,2,4,*]
[1]Trev and Joyce Deeley Research Centre, British Columbia Cancer Agency, Victoria, BC V8R 6V5, Canada
[2]Department of Biochemistry and Microbiology, University of Victoria, Victoria, BC V8W 2Y2, Canada
[3]Research Institute of Molecular Pathology (IMP), Vienna Biocenter (VBC), 1030 Vienna, Austria
[4]Lead Contact
*Correspondence: jjlum@bccancer.bc.ca
http://dx.doi.org/10.1016/j.celrep.2017.04.012

SUMMARY

Citrate is a required carbon precursor for de novo fatty acid and membrane lipid synthesis. However, the pathways regulating intracellular citrate, particularly during the initial transition from a resting state to cell growth, remain unclear. Here, we show that STAT3 is among the first signaling events activated in resting lymphocytes following growth factor stimulation. During this period, the inhibition of STAT3 blocks the expression of citrate synthase (CS) and reduces the levels of intracellular citrate. As a consequence of CS loss and the reduction in citrate, cells are unable to grow or proliferate in response to extracellular growth factors. These effects were due to STAT3-dependent transcriptional regulation of *CS*, as exogenous addition of citrate could restore fatty acid synthesis, cell growth, and proliferation. Taken together, our studies reveal that transcription-dependent control of *CS* is essential for regulating the initiation of cell growth.

INTRODUCTION

In yeast, exit from carbon-withdrawal-induced quiescence relies on glucose catabolism and is independent of ATP production (Laporte et al., 2011). This ensures that cells accumulate sufficient biomass or size before beginning DNA replication and cell division (Fantes and Nurse, 1977; Mitchison and Nurse, 1985; Nurse and Thuriaux, 1977; Werner-Washburne et al., 1993). In contrast, multicellular organisms require extrinsic growth factors to instruct the uptake of extracellular nutrients. The uptake of glucose is crucial for the production of mitochondria-derived citrate, the main metabolic precursor for de novo cytosolic fatty acid synthesis in proliferating cells (Currie et al., 2013; Hatzivassiliou et al., 2005). The dependency on citrate to fuel growth implies that, in addition to maintaining high rates of glycolysis, specific steps of the tricarboxylic acid cycle (TCA) must be coordinately regulated to satisfy the demands for growth. How extrinsic signals control the production of citrate is not known.

The synthesis of glucose-derived citrate is catalyzed by citrate synthase (CS) through the condensation reaction of oxaloacetate with acetyl-CoA. A role for CS in cell growth and proliferation has been observed in algae, plants, yeast, bacteria, and worms, where the absence of CS contributes to defects in meiosis and cell division (Murray and Hynes, 2010; Rahman et al., 2014; Ruprich-Robert et al., 2002; Song et al., 2013; Vandedrinck et al., 2001). In bacteria and plants, citrate is produced during the first growth phase (López-y-López and de la Torre, 2005), and loss of CS causes growth defects and decreased flowering (Landschütze et al., 1995). In addition, acute stimulation of hematopoietic cells with mitogens was found to upregulate CS expression, implying a role for CS in metabolic regulation during early phases of lymphocyte activation (Keast and Newsholme, 1991).

The JAK/STAT signaling pathway is involved in growth factor and gp130-mediated cytokine signaling, both of which are required for activation of key cellular processes such as the cell cycle, survival, and proliferation (Fukada et al., 1996). Previous studies have found that deletion of *STAT3* in T cells resulted in defective IL-6-dependent proliferation (Akaishi et al., 1998). Moreover, the expression of STAT3 is required for both lymphopenia-induced expansion of CD4+ T cells and for a T cell transfer model of colitis, highlighting a crucial role of STAT3 in lymphoproliferative disorders (Durant et al., 2010). One potential explanation for these phenotypic observations is the reported role of STAT3 in the regulation of metabolism. For example, STAT3 has been found to associate with complex I and II of the electron transport chain (Wegrzyn et al., 2009; Zhang et al., 2013). Taken together, these data imply that STAT3 may play an important role in the modulation of growth and proliferation through multiple metabolic mechanisms.

Interleukin-3 (IL-3)-dependent hematopoietic cells deficient for the pro-apoptotic proteins Bax and Bak (DKO cells) survive several weeks and rely on macroautophagy to support survival in the absence of IL-3 (Lum et al., 2005). Upon IL-3 readdition, all cells restore their glycolytic capacity and are able to resume cell growth. This provides a system to examine signaling events that coordinate metabolic reprogramming during the earliest phase of restimulation. STAT3 was among the first transcription factors to be activated following IL-3 readdition. Pharmacological or genetic inhibition of STAT3 blocked IL-3-dependent and T cell receptor (TCR)-induced expression of CS and prevented recovery of cell size and proliferation. During IL-3 readdition, STAT3 bound to a putative consensus sequence on *CS* and activated transcription. Moreover, shRNA knockdown of CS at the time of IL-3 restimulation resulted in the inhibition of cell growth

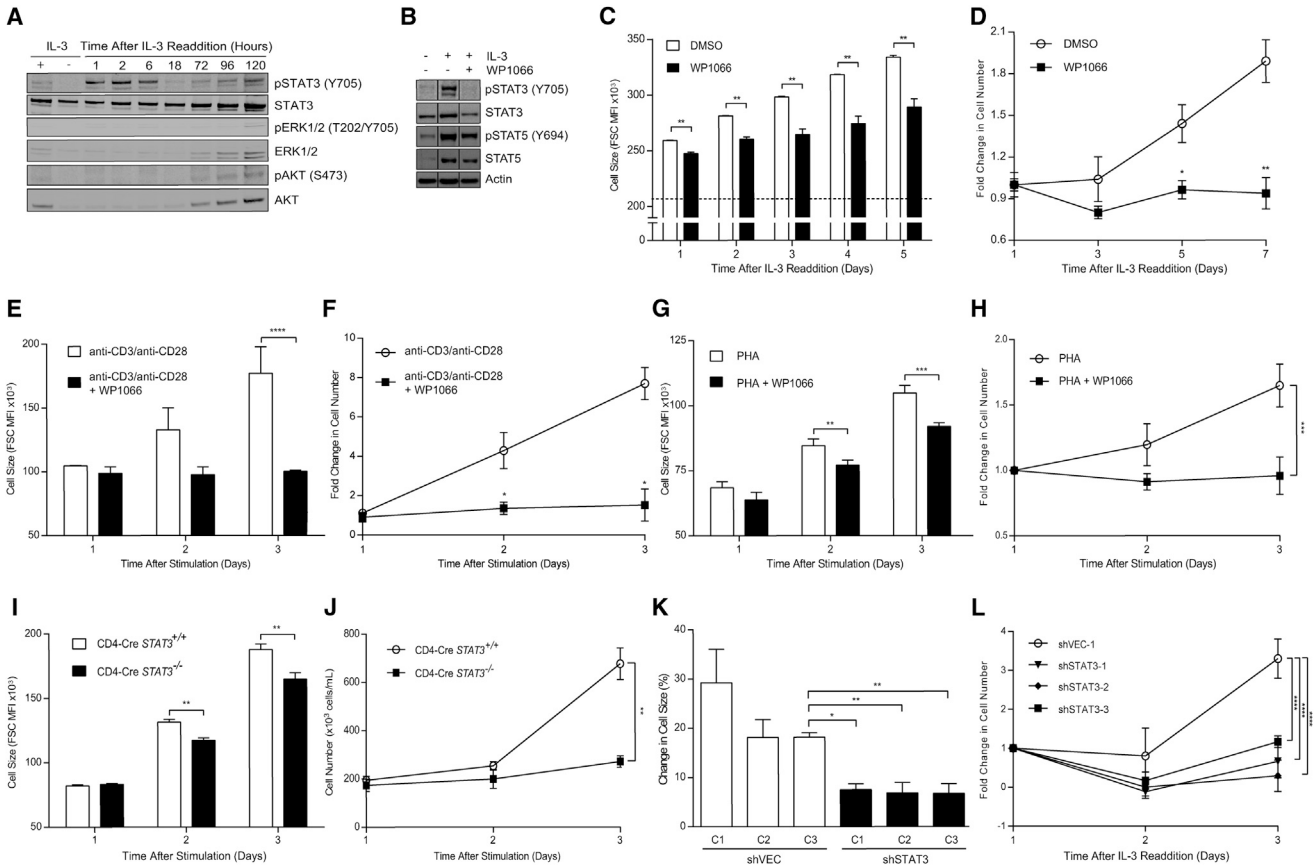

Figure 1. Inhibition of STAT3 Prevents Recovery of Cell Growth and Proliferation in Response to Growth Factor Signaling

(A) Phospho- and total ERK, AKT, and STAT3 activity in DKO cells in the presence of IL-3 (+), 21 days post-IL-3 withdrawal (−), and hours after IL-3 readdition (representative of n = 3).

(B) Phospho- and total STAT3 and STAT5 in 14-day IL-3-deprived DKO cells (−), 24 hr after IL-3 readdition, with or without WP1066 (representative of n = 3).

(C) Cell size measured by forward scatter (FSC) after IL-3 readdition with or without WP1066.

(D) Cell number after IL-3 readdition, with or without WP1066. Fold change was calculated by dividing the IL-3-readdition cell number by the 14 day IL-3-deprived cell number.

(E) Cell size in CD8+ T cells stimulated with anti-CD3/anti-CD28 with or without WP1066.

(F) Cell number of CD8+ T cells stimulated with anti-CD3/anti-CD28 with or without WP1066.

(G) Cell size in human PBMCs stimulated with PHA with or without WP1066.

(H) Cell number of human PBMCs stimulated with PHA with or without WP1066 calculated as in (D).

(I) Cell size in CD4-*Cre STAT3*$^{+/+}$ or CD4-*Cre STAT3*$^{-/-}$ after stimulation.

(J) Cell number of CD4-*Cre STAT3*$^{+/+}$ or CD4-*Cre STAT3*$^{-/-}$ after stimulation.

(K) Change in DKO cell size from 6 to 24 hr in response to IL-3 readdition for three independent shVEC and shSTAT3 clones.

(L) Fold change in DKO cell number in shVEC and three shSTAT3 clones measured days after IL-3 readdition calculated as in (D).

Panels (C), (D), (I), and (J) show average ± SEM (n = 3, Student's t test, *p < 0.05, **p < 0.01). Panels (E)–(H), (K), and (L) show average ± SD (n = 3, one-way ANOVA plus a Dunnet post-test, *p < 0.05, **p < 0.01, ***p < 0.001, ****p < 0.0001).

and proliferation. Taken together, these data demonstrate an essential transcriptional role for STAT3 in the regulation of *CS*-dependent cell growth.

RESULTS

Inhibition of the STAT3 Pathway Prevents Recovery of Cell Growth and Proliferation in Response to Growth Factor Signaling

To investigate the sequence of signaling events that regulate initial cell growth, DKO cells were cultured in the absence of IL-3 for 21 days, and upon IL-3 readdition, the expression of several key regulators of cell growth was examined. STAT3 phosphorylation was detected within the first hour of IL-3 readdition (Figure 1A). In contrast, the phosphorylation of AKT and ERK1/2 did not occur until 72 hr after IL-3 readdition, a time point at which cells have increased in size (Lum et al., 2005).

To study the importance of STAT3 activation on cell growth, DKO cells were treated in the presence or absence of a STAT3 inhibitor (WP1066) upon IL-3 readdition. The activation of STAT3 following IL-3 stimulation was suppressed by treatment with WP1066, while phosphorylation and total STAT5 levels remained

largely unaffected (Figure 1B). Treatment with WP1066 also blocked the recovery of cell size (Figure 1C) and the capacity to proliferate (Figure 1D) in response to IL-3. Resting naive CD8+ T cells isolated from splenocytes and stimulated in vitro with anti-CD3/anti-CD28 were also tested in the presence or absence of WP1066. Consistent with the DKO cells, WP1066 inhibited cell growth and proliferation of activated CD8+ T cells (Figures 1E and 1F). Similarly, in vitro mitogenic stimulation of human PBMCs (peripheral blood mononuclear cells) with phytohaemgglutinin (PHA) in the presence of WP1066 also led to a block in cell growth and proliferation (Figures 1G and 1H). To confirm the intrinsic role of STAT3 on initial cell growth and proliferation, naive splenocytes from CD4-Cre-*STAT3*$^{+/+}$ or -*STAT3*$^{-/-}$ mice were activated in vitro with anti-CD3/anti-CD28. Similar to WP1066, genetic ablation of *STAT3* in CD4+ T cells led to abrogation of cell growth and a complete suppression of proliferation (Figures 1I and 1J).

Finally, an inducible shRNA was used to silence STAT3 to examine its role on cell size and proliferation in the DKO cells. In three independent clones, the knockdown of STAT3 (short hairpin STAT3, shSTAT3) resulted in the inability to regain cell size and proliferation compared to the shVEC (short hairpin vector control) cells (Figures 1K and 1L). These effects of STAT3 are specific to initial cell growth, as there was no difference in the growth or proliferation of shSTAT3 cells cultured in the continued presence of IL-3 (Figures S1A and S1B). Furthermore, constitutively active STAT3 was found to promote cell growth, as DKO cells displayed a greater than 2.5-fold increase in the recovery of cell size compared to the vector control cells during IL-3 readdition (Figures S1C and S1D).

Suppression of STAT3 Results in Decreased Mitochondrial Membrane Potential, CS Expression, and Citrate Levels

Recent work has suggested that STAT3 regulates cellular metabolism through its localization within the mitochondria. Mitochondrial STAT3 is thought to have a direct regulatory role in oxidative metabolism and electron transport due to the decrease in complex I and II activity observed in *STAT3*$^{-/-}$ cells (Wegrzyn et al., 2009). To determine the effects of STAT3 inhibition on mitochondrial function, flow cytometric analysis of mitochondrial repolarization was measured by tetramethylrhodamine ethyl ester (TMRE). Compared to control treatment, IL-3-deprived cells had a significant impairment in their recovery of mitochondrial potential after IL-3 readdition in the presence of WP1066 (Figures 2A, 2B, and S2A). This was not due to a loss in mitochondrial mass, as there was no difference in Mitotracker staining (Figure 2C). The effect of WP1066-mediated inhibition of STAT3 on cell size was also not due to defects in electron transport chain activity, as inhibition of complex I with rotenone or complex II with TTFA caused a reduction in TMRE, but neither drug had an effect on the recovery of cell size following IL-3 readdition (Figures S2B and S2C).

The block in both cell size and mitochondrial membrane potential recovery with WP1066 led to the speculation that STAT3 controls the level of metabolites for de novo fatty acid synthesis. Citrate is found at a crucial point in the TCA cycle, where it can serve as an important precursor for cytosolic acetyl-CoA and subsequent fatty acid synthesis or be converted to α-ketoglutarate for further oxidation. Thus, the level of citrate may be an important rheostat-controlling anabolism versus catabolism. To determine whether STAT3 can regulate this central metabolite, intracellular citrate was measure in DKO cells that were treated in the presence or absence of WP1066 at the time of IL-3 readdition. By 48 hr after IL-3 readdition, citrate had recovered to levels similar to cells cultured in the continued presence of IL-3. In contrast, the inhibition of STAT3 with WP1066 led to a dramatic loss in the ability to accumulate citrate over the same time course (Figure 2D). The reduction in total citrate levels suggested that the expression of STAT3 regulates the production of citrate. Indeed, *CS* mRNA levels increased 5-fold following IL-3 readdition, but this upregulation was blocked in the presence of WP1066 (Figure 2E). Consistent with this, immunoblotting revealed that, between 24 hr and 48 hr after IL-3 readdition, the amount of CS protein increased, but this was suppressed in the presence of WP1066 (Figure S2D). The expression of CS was also suppressed in stimulated T cells treated with WP1066 (Figure S2E), as well as in TCR-stimulated CD4-Cre-*STAT3*$^{-/-}$ cells (Figures S2F and S2G).

The loss in the re-expression of CS was further confirmed in shSTAT3 DKO cells following IL-3 readdition (Figure 2F). The effect of STAT3 on CS is specific to the period of cell growth immediately after IL-3 stimulation, as there was no difference in the expression of CS in shSTAT3 cells cultured in the continued presence of IL-3 (Figure S2H). As a consequence of the impaired recovery of CS expression in shSTAT3 DKO cells, there was a dramatic reduction in the total intracellular citrate levels following IL-3 readdition (Figure 2G). In addition, the recovery in intracellular citrate levels following IL-3 readdition in DKO cells was unaffected by complex I or complex II inhibitors (Figure S2I), implying that cell growth under these conditions was independent of electron transport chain activity. Taken together, these data suggest that STAT3 controls CS expression during the initiation of cell growth and that this effect is not limited to IL-3-dependent DKO cells.

Direct Regulation of CS by STAT3 during IL-3 Recovery

To examine whether *CS* is a direct transcriptional target of STAT3, an in silico bioinformatic analysis was performed to identify potential STAT3 consensus sites on the *CS* promoter. This analysis revealed a putative STAT3 binding site located 54 bps downstream of the CS start codon. Chromatin immunoprecipitation (ChIP) was conducted to assess whether STAT3 could bind to this site in response to IL-3 readdition. In IL-3-deprived cells, there was no association of STAT3 or STAT5 to the putative binding site. However, within 4 hr of IL-3 readdition, there was a 3-fold increase in bound STAT3 to the putative STAT3 site (Figures 3A and 3B).

To determine if this STAT3 binding site could promote gene transcription in response to IL-3 stimulation, a luciferase reporter containing the wild-type (WT) or a mutant (MT) STAT3 binding site was generated. In response to IL-3 readdition, there was a 4-fold increase in luciferase activity in cells transfected with the STAT3 WT binding site compared to cells transfected with the STAT3 MT or cells that contained the empty vector (Figure 3C).

Multiple studies have shown that STAT3 can function in the absence of its transcriptional activity (Macias et al., 2014;

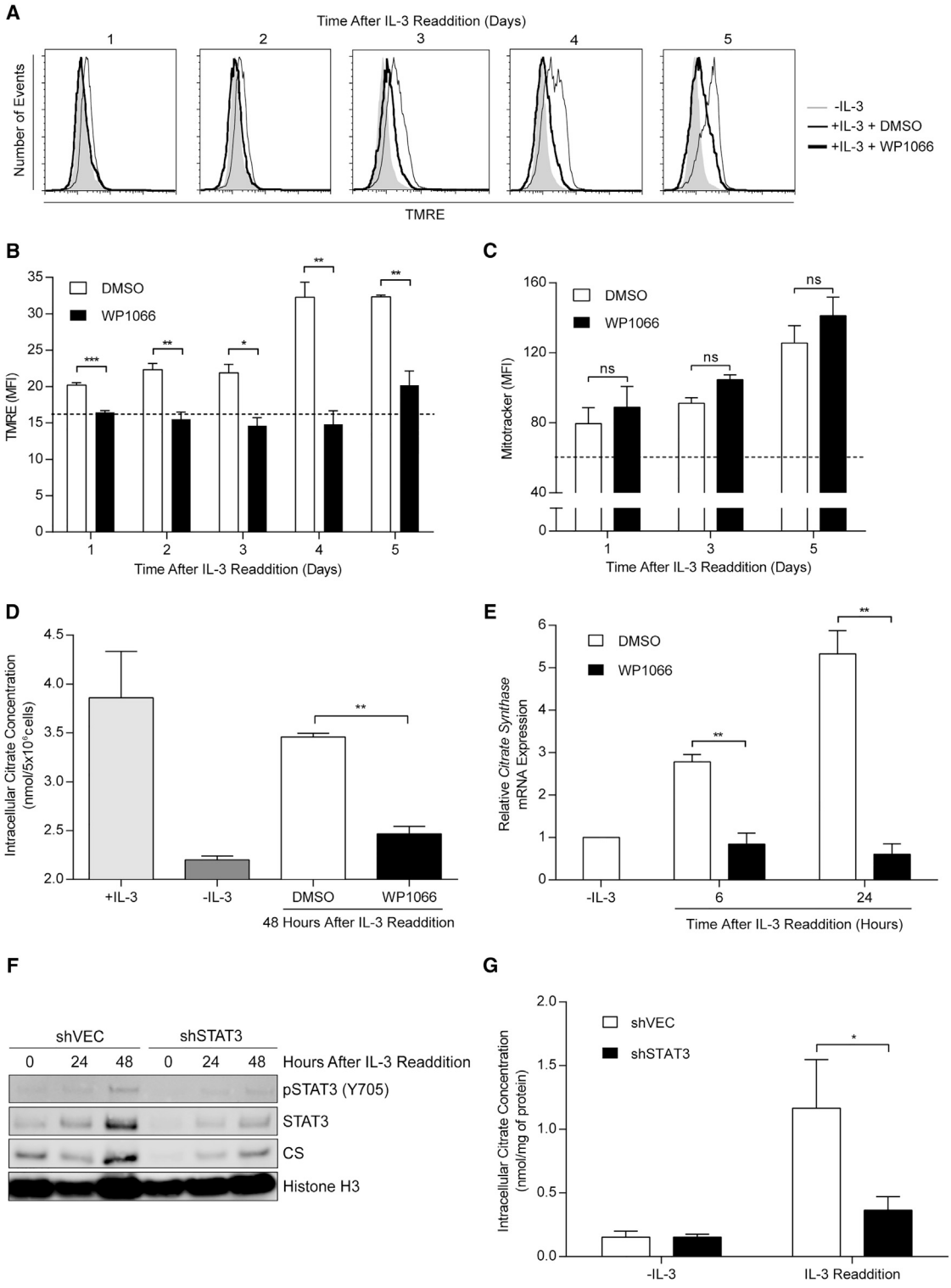

Figure 2. STAT3 Inhibition Blocks the Recovery of Mitochondrial Membrane Potential, Citrate Synthase Expression, and Citrate

(A) Mitochondrial membrane potential measured by TMRE in DKO cells cultured in the absence of IL-3 for 14 days (gray-filled histogram), after IL-3 readdition with or without WP1066 (representative of n = 3).

(B) Quantification of the TMRE staining, as shown in (A). MFI, mean fluorescent intensity.

(C) Mitochondrial mass days after IL-3 readdition with or without WP1066.

(legend continued on next page)

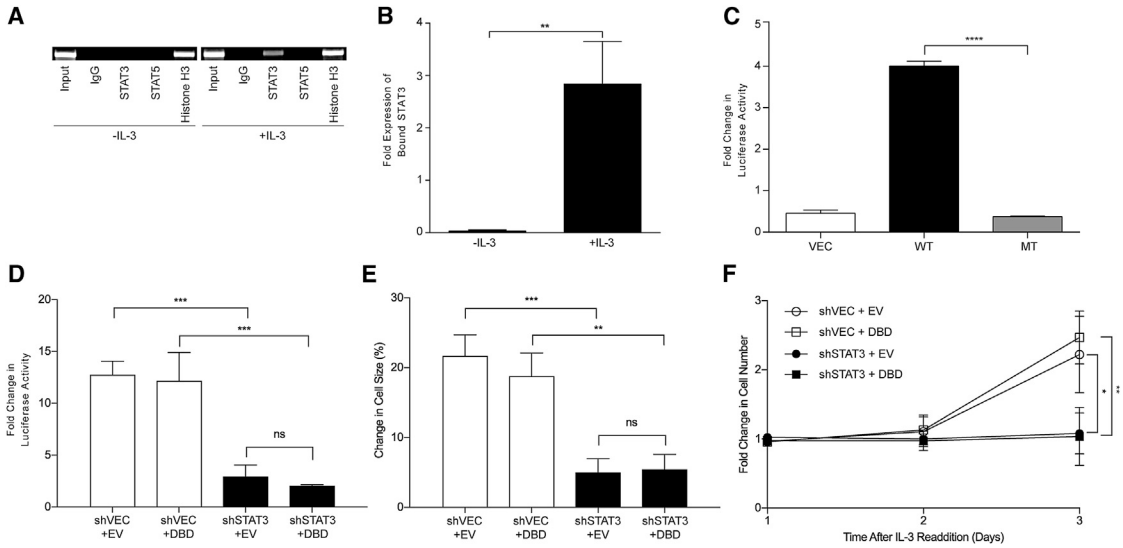

Figure 3. STAT3 Transcriptionally Regulates Expression of Citrate Synthase during Early IL-3 Recovery

(A) DKO cells were starved for 14 days; 4 hr after IL-3 readdition, cell lysates were analyzed for STAT3 binding by ChIP (representative of n = 3).

(B) Quantification of ChIP PCR from (A).

(C) STAT3 luciferase reporter activity 6 hr after IL-3 readdition. Fold change in luciferase in the empty vector control (VEC), the wild-type (WT), and the mutant binding site (MT). Graph shows average ± SEM (n = 3, Student's t test, ****$p < 0.0001$).

(D and E) (D) STAT3 reporter activity or (E) change in DKO cell size from 6 to 24 hr in response to IL-3 readdition for shVEC and shSTAT3 cells reconstituted with transcriptionally inactive STAT3 (DBD) or empty vector (EV).

(F) Fold change in DKO cell number for shVEC and shSTAT3 cells expressing DBD or EV. Fold change was calculated by dividing the IL-3 readdition cell number by the IL-3-deprived cell number. Panels (B) and (D)–(F) show average ± SD (n = 3, one-way ANOVA plus a Dunnet post-test; *$p < 0.05$, **$p < 0.01$, ***$p < 0.001$).

Tammineni et al., 2013). To address this possibility in greater detail, a *STAT3* DNA-binding domain (DBD) construct containing a five-amino-acid mutation or empty vector (EV) was expressed in both shVEC and shSTAT3 cell lines. This mutation has no effect on STAT3 phosphorylation and dimerization but leads to the inability to bind DNA (Horvath et al., 1995). Upon IL-3 readdition, the shSTAT3 + DBD cells displayed minimal luciferase reporter activity compared to shVEC + DBD-expressing cells (Figure 3D) despite detection of STAT3 protein in cells expressing the DBD mutant (Figure S2J). Consistent with this, DKO cells expressing the shSTAT3 + DBD were unable to grow and proliferate (Figures 3E and 3F). These data imply that the recovery of cell growth and proliferation in response to IL-3 requires transcriptionally active STAT3.

Loss of CS Expression Impairs Recovery of Cell Growth and Proliferation

The enzymatic product of CS, citrate, can remain in the mitochondria for subsequent oxidation or be exported to the cytosol for fatty acid biosynthesis. To test whether the loss in CS would impair initial cell growth, DKO cells expressing an inducible shCS (short hairpin citrate synthase) or control shVEC were generated and starved for 14 days. Upon IL-3 readdition, shCS cells showed a significant reduction in CS expression and total levels of intracellular citrate compared to control cells (Figures S3A and S3B). The loss in CS expression and citrate levels resulted in a dramatic impairment in the recovery of cell size and proliferation following IL-3 readdition (Figures S3C and S3D). Like the STAT3 knockdown, the effect of CS suppression was specific to the earliest period of cell growth, as there was no influence on cell size or number in shCS cells cultured in the continuous presence of IL-3 (Figures S3E–S3G).

Citrate Supports De Novo Fatty Acid Synthesis

The inability to recover cell size due to the loss of STAT3-mediated expression of CS is likely a consequence of the subsequent decline in available citrate for production of fatty acids. To demonstrate this, the amount of incorporation of ^{14}C-glucose and ^{14}C-citrate carbon into fatty acids was measured in the shSTAT3 cells during IL-3 readdition. In contrast to shVEC cells, there was minimal incorporation of ^{14}C into total cellular lipids in the shSTAT3 cells during the first 24 hr of IL-3 readdition using

(D) Intracellular citrate levels in DKO cells in the presence of IL-3, 14 days post-IL-3 withdrawal, and 48 hr after IL-3 readdition with or without WP1066.

(E) Relative CS mRNA expression 14 days post-IL-3 withdrawal (-IL-3) and hours after IL-3 readdition with or without WP1066. Panels (B)–(E) show average ± SEM (n = 3, Student's t test; *$p < 0.05$, **$p < 0.01$, ***$p < 0.001$).

(F) Levels of phospho- and total STAT3 and CS 14 days post IL-3 withdrawal and hours after IL-3 readdition in shVEC or shSTAT3 cells (representative of n = 3).

(G) Intracellular citrate levels in shVEC or shSTAT3 cells 14 days post-IL-3 withdrawal and 24 hr after IL-3 readdition. Graph shows average ± SD (n = 3, one-way ANOVA plus a Dunnet post-test; *$p < 0.05$).

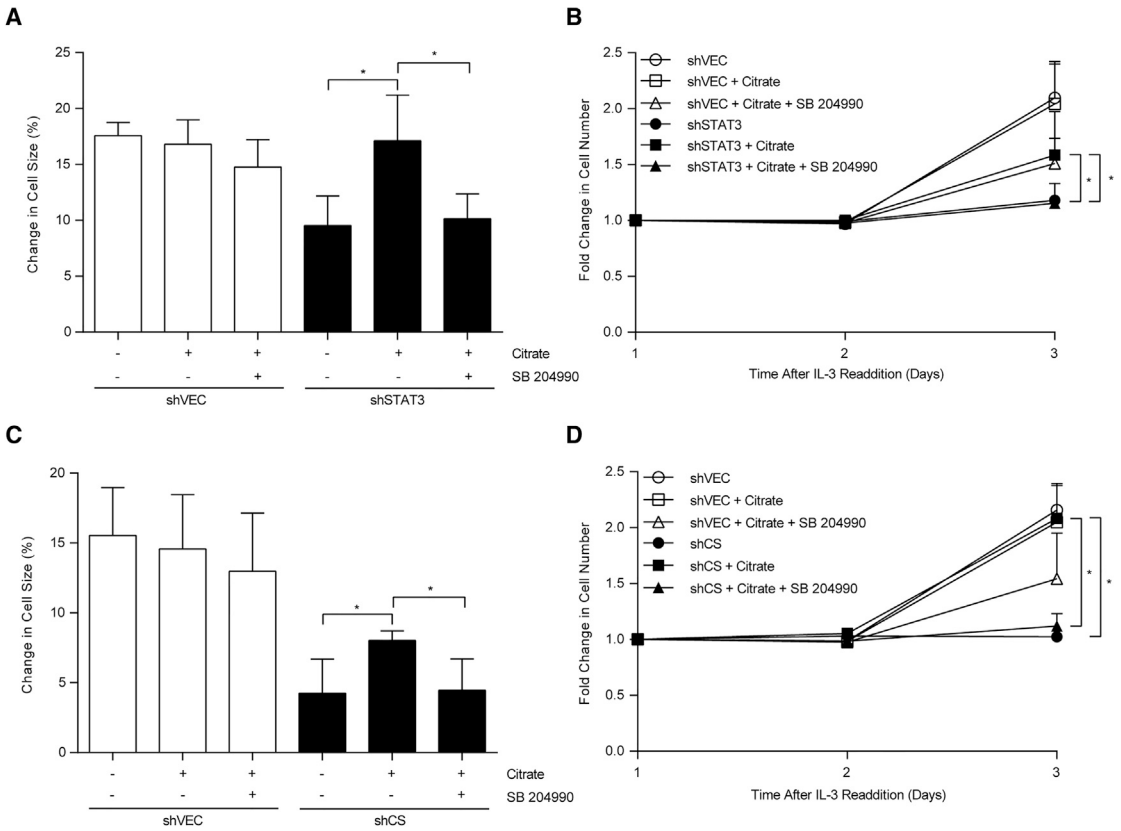

Figure 4. Loss in Cell Growth and Proliferation by shSTAT3 or shCS Can Be Rescued by Exogenous Citrate

(A) Change in cell size from 6 to 24 hr in shVEC and shSTAT3 cells, with (+) or without (−) exogenous sodium citrate and SB 204990, at the time of IL-3 readdition.

(B) Fold change in DKO cell number after IL-3 readdition in shVEC and shSTAT3 cells, with or without sodium citrate and SB 204990, at the time of IL-3 readdition. Fold change was calculated by dividing the IL-3 readdition cell number by the IL-3-deprived cell number.

(C) Change in cell size from 6 to 24 hr in shVEC and shCS cells as described in (A).

(D) Fold change in DKO cell number after IL-3 readdition in shVEC and shCS cells as described in (B).

Panels (A)–(D) show average ± SD (n = 3, one-way ANOVA plus a Tukey's post-test; *p < 0.05).

glucose as a precursor (Figure S4A). As expected, the amount of lipid synthesis from ^{14}C-citrate was similar between shVEC and shSTAT3 cells since exogenously labeled ^{14}C-citrate can bypass CS and incorporate directly into fatty acids (Figure S4B). Together, this confirms that STAT3 regulation of CS and subsequent production of glucose-derived citrate contribute to fatty acid synthesis during IL-3 readdition.

Loss in Cell Growth and Proliferation by STAT3 or CS Knockdown Can Be Rescued by Exogenous Citrate

The above results suggest that STAT3 is involved in the transcriptional regulation of *CS* and that this is crucial for citrate-derived production of fatty acids during IL-3 restimulation. To support these findings, we attempted to rescue the loss in cell size and proliferation seen in the shSTAT3 and shCS cell lines with citrate during IL-3 readdition. The addition of exogenous citrate to shSTAT3 and shCS cells rescued cell size and proliferation (Figures 4A–4D). To further demonstrate that citrate contributes to fatty acid synthesis for cell growth, an ATP citrate lyase inhibitor (SB 204990) was used at the time of IL-3 readdition to block the cytosolic conversion of citrate to acetyl-CoA and hence fatty acid synthesis (Hatzivassiliou et al., 2005). As shown in Figures 4A–4D, upon IL-3 readdition, shSTAT3 and shCS cells were unable to initiate either cell growth or proliferation in the presence of SB 204990. Therefore, in the absence of CS or STAT3, exogenous citrate can support cell growth and proliferation.

DISCUSSION

STAT3 Regulates Growth and Proliferation

Based on the above results, resting lymphocytes require STAT3 expression to restore cell growth and proliferation. The preservation of STAT3 expression during periods of starvation may serve to ensure that cells can respond to lineage-dependent growth factor restimulation, even after extended periods of IL-3 deprivation (Lum et al., 2005). However, the metabolic role of STAT3 appears to be important only during the initial stages after growth factor stimulation, since suppression of STAT3 had no impact on growth or proliferation of exponentially growing cells. This suggests that other signaling pathways may provide redundancy to ensure that growth-dependent programs are sustained once cells have entered the cell cycle. At least for STAT5, PI3K/AKT,

and MAP/ERK, these pathways are not involved in the early cell growth but rather their expression appears to be more critical after cells have already initiated cell growth.

STAT3 was originally identified as an acute phase response factor that binds to IL-6 responsive *cis*-acting elements (Kordula and Travis, 1996). Subsequent loss-of-function studies found that STAT3 was required for growth, proliferation, and suppression of apoptosis in response to in vitro stimulation with a broad range of cytokines and growth factors (Bromberg and Darnell, 2000; Fukada et al., 1996). These defects in growth and proliferation are most clearly observed in mice deficient in STAT3, but not other STAT members, where *STAT3* knockout mice die during early embryogenesis. The wide-ranging cell types affected by lineage-dependent STAT3 signaling may also explain why it plays a more prominent role in the coordination of metabolism than previously appreciated. Although STAT5 is also activated by IL-3, the appearance of phospho-STAT5 occurred subsequent to the observed changes in cell size, implying a less crucial role in early cell growth.

CS Is a Conserved Pathway for Growth and Division

Glucose-derived citrate can be exported into the cytosol for de novo fatty acid synthesis or oxidized to produce NADH via the TCA cycle. For this reason, the intracellular level of citrate is a central point of regulation for anabolic or catabolic metabolism in the cell. Upon growth factor stimulation, CS expression increases concurrently with the activation of STAT3. During this period, loss of CS results in a dramatic reduction in the intracellular levels of citrate. As a consequence, there was a complete suppression in cell growth and an inability to initiate proliferation. Similarly, in yeast, *E. coli*, and *C. elegans*, growth and division in response to nutrients is dependent on CS (Murray and Hynes, 2010; Rahman et al., 2014; Ruprich-Robert et al., 2002; Song et al., 2013; Vandedrinck et al., 2001). In addition, overexpression of CS can increase the production of citrate and promote cell growth in *A. thaliana* and *E. coli* (Koyama et al., 2000; Vandedrinck et al., 2001).

In the absence of STAT3, exogenous citrate rescued cell growth and proliferation during IL-3 readdition. Another potential way to bypass the suppression of cell growth in STAT3-deficient cells is supplementation of exogenous fatty acids such as palmitate. Of note, neither α-ketaglutarate nor acetate could recover growth and proliferation in cells lacking STAT3 (data not shown). The reason for this is unclear, though it is possible that, during the first few days of IL-3 readdition, the expression of isocitrate dehydrogenase and acetyl-CoA synthetase had not yet recovered to levels required to support the utilization of these carbon sources. Moreover, the acute re-expression of CS may serve an additional role in supporting fatty acid synthesis and cell growth. For instance, feedback inhibition of phosphofructose kinase 1 via citrate would allow carbons from glucose to be redirected toward the pentose phosphate pathway. This would in turn generate the required NADPH to facilitate de novo fatty acid synthesis from citrate. Although these are plausible scenarios to consider, they will require additional investigation. Nonetheless, the conserved metabolic function of STAT3 on the regulation CS supports its role in providing carbon substrates to enable resting cells to resume growth and proliferation.

EXPERIMENTAL PROCEDURES

Cell Culture and T Cell Isolation

IL-3-dependent $Bax^{-/-}$ $Bak^{-/-}$ hematopoietic cells (DKO) were cultured as previously described (Lum et al., 2005). CD8+ and CD4+ splenocytes (from CD4-Cre $STAT3^{+/+}$, $STAT3^{-/-}$; gift from Dr. John O'Shea) were purified by negative selection (Miltenyi Biotec) or EasySep (StemCell Technologies, Inc.) and cultured in standard RPMI 1640 media supplemented with 100 IU IL-2 (eBioscience) containing plate bound anti-CD3 (1 μg/mL) and anti-CD28 (0.5 μg/mL) (BD PharMingen). Human PBMCs were commercially obtained from leukopaks (STEMCELL) and were cultured in standard RPMI 1640 media supplemented with 1 μg/mL PHA (Sigma-Aldrich) and 50 IU IL-2 (eBioscience). Unless otherwise indicated, DKO IL-3 withdrawal periods were 14 days, and knockdown was induced by the addition of doxycycline (Dox) 2 days prior to IL-3 readdition. Mice were female C57BL/6 at least 8 weeks of age, and animal studies were approved by the UVIC Animal Care Committee. $STAT3^{-/-}$ mice were maintained according to the NIH guidelines for the use and care of live animals with the approval by the Institutional Animal Care and Use Committee of NIAMS.

Reagents

Citrate assay was conducted following the manufacturer's protocol (Abcam). Trypan blue exclusion (Sigma-Aldrich) or 123-count eBeads (eBioscience) were used for determining cell numbers. The reagents used include sodium citrate (20 mM; Sigma-Aldrich), WP1066 (8 μM; Calbiochem), ATP citrate lyase inhibitor, SB 204990 (25 μM; Tocris), Rotenone (1 ng/mL; Sigma-Aldrich), and thenoyltrifluoroacetone (25 μM TTFA; Cayman Chemical).

Flow Cytometry

Mitochondrial membrane potential was measured using TMRE (10 nM) and CCP (5 nM). Mitochondrial mass was measured by staining cells with Mitotracker Green FM (10 nM) (Invitrogen). All data were collected on a BD FACSCalibur and analyzed using FlowJo Data analysis Software (Tree Star Inc.).

Immunoblotting

Cells were lysed with RIPA buffer, resolved on a NuPAGE 4%–12% BisTris gel (Invitrogen), and then transferred onto nitrocellulose membrane (Life Sciences). The following antibodies were used (all 1:1,000): pStat3 (Y705), Stat3, pStat5 (Y694), Stat5, pAkt (S473), Akt, pERK1/2 (T202/Y705), ERK1/2 (Cell Signaling), CS, Histone H3 (Abcam), and β-actin (Sigma-Aldrich). Secondary antibodies were used at either 1:10,000 anti-rabbit or 1:10,000 anti-mouse IRDye 800 (Rockland), followed by imaging (LiCOR Odyssey) and quantification using ImageJ.

Quantitative PCR

RNA isolation and cDNA synthesis were carried out using the RNeasy Plus Mini kit (QIAGEN) and Quanta cDNA synthesis kit. qPCR was performed with a MyiQ system (Bio-Rad). Primers: STAT3 F:CTGGCGGGGCTCTTGTCAGC, R:TGACTAAGGGCCGGTCCGGG; CS F:GCCCAAGTCCATGAGCACGGA, R:CCACATGCTTCAGTCCCGGTCA.

Chromatin Immunoprecipitation

Cells were treated with formaldehyde and sonicated (4 cycles of 15, 1 s pulse). Antibodies used: IgG (Cell Signaling; 1 μL), Histone H3 (Cell Signaling; 3 μL), STAT3, and STAT5 (Cell Signaling; 5 μL). Protein A beads were incubated with the samples for 1 hr at 4°C followed by chelex bead DNA enrichment. For detection of targets, the following primer pairs were used: CS F: AAAGCC AGGAGACCTTGATG, R: CCCAAACAAGAAACAAAGGAAGA.

shRNA, STAT3 WT and MT Vectors, and Luciferase Assay

A doxycycline (Dox)-induced Tet-ON system was used to generate the knockdown cell lines (Zuber et al., 2011), as well as a constitutive STAT3-expressing cell line. The DNA-binding domain mutant was kindly provided by Dr. Lee (Wang et al., 2011) and cloned into MSCV-Thy1.1. The MSC-Thy1.1-STAT3 was a gift from Dr. Mark Kaplan. Viral particles were generated as per Swift et al., 2001. The STAT3 WT and MT binding site luciferase constructs were generated by modifying four consecutive nucleotides in the sequence flanked by the STAT3 consensus sequence (WT:CCTTCCCGCCAG; MT: CCTggaa

GCCAG). Luciferase assays were performed by transfection of a renilla control and firefly target constructs. Transfected DKO cells were incubated in complete media containing IL-3 for 2 days before a 14 day IL-3 withdrawal. Lysates were harvested 6 hr post-IL-3 readdition and luciferase quantified as per the manufacturer's protocol (Promega) using an EnVision plate reader (PerkinElmer).

^{14}C Glucose and Citrate Labeling

At the time of IL-3 readditions, cells were incubated with U-[^{14}C]-glucose or U-[^{14}C]-citrate (Perkin Elmer), and lipid synthesis was measured as previously described (Lum et al., 2007).

Statistical Analysis

All statistical calculations were used using GraphPad 6.0 software; p values < 0.05 were considered significant.

SUPPLEMENTAL INFORMATION

Supplemental Information includes four figures and can be found with this article online at http://dx.doi.org/10.1016/j.celrep.2017.04.012.

AUTHOR CONTRIBUTIONS

J.J.L. conceptualized and S.M. and M.H. conducted the project. J.J.L., S.M., M.H., and C.G. performed the experiments. J.J.L., S.M., M.H., T.H., and J.Z. aided in experimental design and scientific suggestions. All authors edited the manuscript.

ACKNOWLEDGMENTS

The authors would like to thank Dr. John O'Shea and Dr. Yuka Kanno for the CD4-Cre-STAT3 knockout spleens and Dr. Lindsay DeVorkin and Dr. David Kroeger for their advice. The work in this manuscript was supported by (all to J.J.L.) the BC Cancer Foundation, the Cancer Research Society, and the Canadian Institutes of Health Research. S.M. was partially supported by a scholarship from the University of Victoria.

Received: March 22, 2016
Revised: March 7, 2017
Accepted: April 4, 2017
Published: May 2, 2017

REFERENCES

Akaishi, H., Takeda, K., Kaisho, T., Shineha, R., Satomi, S., Takeda, J., and Akira, S. (1998). Defective IL-2-mediated IL-2 receptor alpha chain expression in Stat3-deficient T lymphocytes. Int. Immunol. *10*, 1747–1751.

Bromberg, J., and Darnell, J.E., Jr. (2000). The role of STATs in transcriptional control and their impact on cellular function. Oncogene. *19*, 2468–2473.

Currie, E., Schulze, A., Zechner, R., Walther, T.C., and Farese, R.V., Jr. (2013). Cellular fatty acid metabolism and cancer. Cell Metab. *18*, 153–161.

Durant, L., Watford, W.T., Ramos, H.L., Laurence, A., Vahedi, G., Wei, L., Takahashi, H., Sun, H.W., Kanno, Y., Powrie, F., and O'Shea, J.J. (2010). Diverse targets of the transcription factor STAT3 contribute to T cell pathogenicity and homeostasis. Immunity *32*, 605–615.

Fantes, P., and Nurse, P. (1977). Control of cell size at division in fission yeast by a growth-modulated size control over nuclear division. Exp. Cell Res. *107*, 377–386.

Fukada, T., Hibi, M., Yamanaka, Y., Takahashi-Tezuka, M., Fujitani, Y., Yamaguchi, T., Nakajima, K., and Hirano, T. (1996). Two signals are necessary for cell proliferation induced by a cytokine receptor gp130: involvement of STAT3 in anti-apoptosis. Immunity *5*, 449–460.

Hatzivassiliou, G., Zhao, F., Bauer, D.E., Andreadis, C., Shaw, A.N., Dhanak, D., Hingorani, S.R., Tuveson, D.A., and Thompson, C.B. (2005). ATP citrate lyase inhibition can suppress tumor cell growth. Cancer Cell *8*, 311–321.

Horvath, C.M., Wen, Z., and Darnell, J.E., Jr. (1995). A STAT protein domain that determines DNA sequence recognition suggests a novel DNA-binding domain. Genes Dev. *9*, 984–994.

Keast, D., and Newsholme, E.A. (1991). Effect of B- and T-cell mitogens on the maximum activities of hexokinase, lactate dehydrogenase, citrate synthase and glutaminase in bone marrow cells and thymocytes of the rat during four hours of culture. Int. J. Biochem. *23*, 823–826.

Kordula, T., and Travis, J. (1996). The role of Stat and C/EBP transcription factors in the synergistic activation of rat serine protease inhibitor-3 gene by interleukin-6 and dexamethasone. Biochem. J. *313*, 1019–1027.

Koyama, H., Kawamura, A., Kihara, T., Hara, T., Takita, E., and Shibata, D. (2000). Overexpression of mitochondrial citrate synthase in Arabidopsis thaliana improved growth on a phosphorus-limited soil. Plant Cell Physiol. *41*, 1030–1037.

Landschütze, V., Willmitzer, L., and Müller-Röber, B. (1995). Inhibition of flower formation by antisense repression of mitochondrial citrate synthase in transgenic potato plants leads to a specific disintegration of the ovary tissues of flowers. EMBO J. *14*, 660–666.

Laporte, D., Lebaudy, A., Sahin, A., Pinson, B., Ceschin, J., Daignan-Fornier, B., and Sagot, I. (2011). Metabolic status rather than cell cycle signals control quiescence entry and exit. J. Cell Biol. *192*, 949–957.

López-y-López, V.E., and de la Torre, M. (2005). Redirection of metabolism during nutrient feeding in fed-batch cultures of Bacillus thuringiensis. Appl. Microbiol. Biotechnol. *67*, 254–260.

Lum, J.J., Bauer, D.E., Kong, M., Harris, M.H., Li, C., Lindsten, T., and Thompson, C.B. (2005). Growth factor regulation of autophagy and cell survival in the absence of apoptosis. Cell *120*, 237–248.

Lum, J.J., Bui, T., Gruber, M., Gordan, J.D., DeBerardinis, R.J., Covello, K.L., Simon, M.C., and Thompson, C.B. (2007). The transcription factor HIF-1α plays a critical role in the growth factor-dependent regulation of both aerobic and anaerobic glycolysis. Genes Dev. *21*, 1037–1049.

Macias, E., Rao, D., Carbajal, S., Kiguchi, K., and DiGiovanni, J. (2014). Stat3 binds to mtDNA and regulates mitochondrial gene expression in keratinocytes. J. Invest. Dermatol. *134*, 1971–1980.

Mitchison, J.M., and Nurse, P. (1985). Growth in cell length in the fission yeast Schizosaccharomyces pombe. J. Cell Sci. *75*, 357–376.

Murray, S.L., and Hynes, M.J. (2010). Metabolic and developmental effects resulting from deletion of the citA gene encoding citrate synthase in Aspergillus nidulans. Eukaryot. Cell *9*, 656–666.

Nurse, P., and Thuriaux, P. (1977). Controls over the timing of DNA replication during the cell cycle of fission yeast. Exp. Cell Res. *107*, 365–375.

Rahman, M.M., Rosu, S., Joseph-Strauss, D., and Cohen-Fix, O. (2014). Down-regulation of tricarboxylic acid (TCA) cycle genes blocks progression through the first mitotic division in Caenorhabditis elegans embryos. Proc. Natl. Acad. Sci. USA *111*, 2602–2607.

Ruprich-Robert, G., Zickler, D., Berteaux-Lecellier, V., Vélot, C., and Picard, M. (2002). Lack of mitochondrial citrate synthase discloses a new meiotic checkpoint in a strict aerobe. EMBO J. *21*, 6440–6451.

Song, P., Li, L., and Liu, J. (2013). Proteomic analysis in nitrogen-deprived Isochrysis galbana during lipid accumulation. PLoS ONE *8*, e82188.

Swift, S., Lorens, J., Achacoso, P., and Nolan, G.P. (2001). Rapid production of retroviruses for efficient gene delivery to mammalian cells using 293T cell–based systems. In Curr. Protoc. Immunol. (John Wiley and Sons), pp. 10.17.14–10.17.29.

Tammineni, P., Anugula, C., Mohammed, F., Anjaneyulu, M., Larner, A.C., and Sepuri, N.B.V. (2013). The import of the transcription factor STAT3 into mitochondria depends on GRIM-19, a component of the electron transport chain. J. Biol. Chem. *288*, 4723–4732.

Vandedrinck, S., Deschamps, G., Sablon, E., and Vandamme, E.J. (2001). Metabolic engineering of Escherichia coli: construction and characterization of a gltA (citrate synthase) knockout mutant. Meded Rijksuniv Gent Fak Landbouwkd Toegep Biol Wet *66* (*3a*), 333–336.

Wang, W.-B., Levy, D.E., and Lee, C.-K. (2011). STAT3 negatively regulates type I IFN-mediated antiviral response. J. Immunol. *187*, 2578–2585.

Wegrzyn, J., Potla, R., Chwae, Y.-J., Sepuri, N.B.V., Zhang, Q., Koeck, T., Derecka, M., Szczepanek, K., Szelag, M., Gornicka, A., et al. (2009). Function of mitochondrial Stat3 in cellular respiration. Science *323*, 793–797.

Werner-Washburne, M., Braun, E., Johnston, G.C., and Singer, R.A. (1993). Stationary phase in the yeast Saccharomyces cerevisiae. Microbiol. Rev. *57*, 383–401.

Zhang, Q., Raje, V., Yakovlev, V.A., Yacoub, A., Szczepanek, K., Meier, J., Derecka, M., Chen, Q., Hu, Y., Sisler, J., et al. (2013). Mitochondrial localized Stat3 promotes breast cancer growth via phosphorylation of serine 727. J. Biol. Chem. *288*, 31280–31288.

Zuber, J., McJunkin, K., Fellmann, C., Dow, L.E., Taylor, M.J., Hannon, G.J., and Lowe, S.W. (2011). Toolkit for evaluating genes required for proliferation and survival using tetracycline-regulated RNAi. Nat. Biotechnol. *29*, 79–83.